Rapid Communications

Low-high voltage duality in tunneling spectroscopy of the Sachdev-Ye-Kitaev model

N. V. Gnezdilov, J. A. Hutasoit, and C. W. J. Beenakker
Instituut-Lorentz, Universiteit Leiden, P.O. Box 9506, 2300 RA Leiden, The Netherlands

(Received 30 July 2018; published 31 August 2018)

The Sachdev-Ye-Kitaev (SYK) model describes a strongly correlated metal with all-to-all random interactions (average strength J) between N fermions (complex Dirac fermions or real Majorana fermions). In the large-N limit a conformal symmetry emerges that renders the model exactly soluble. Here we study how the non-Fermi-liquid behavior of the closed system in equilibrium manifests itself in an open system out of equilibrium. We calculate the current-voltage characteristic of a quantum dot, described by the complex-valued SYK model, coupled to a voltage source via a single-channel metallic lead (coupling strength Γ). A one-parameter scaling law appears in the large-N conformal regime, where the differential conductance $G = dI/dV$ depends on the applied voltage only through the dimensionless combination $\xi = eVJ/\Gamma^2$. Low and high voltages are related by the duality $G(\xi) = G(\pi/\xi)$. This provides for an unambiguous signature of the conformal symmetry in tunneling spectroscopy.

DOI: 10.1103/PhysRevB.98.081413

Introduction. The Sachdev-Ye-Kitaev (SYK) model, a fermionic version [1] of a disordered quantum Heisenberg magnet [2,3], describes how N fermionic zero-energy modes are broadened into a band of width J by random infinite-range interactions. The phase diagram of the SYK Hamiltonian can be solved exactly in the large-N limit [4–6], when a conformal symmetry emerges at low energies that forms a holographic description of the horizon of an extremal black hole in a (1+1)-dimensional anti–de Sitter space [1,3,4,7].

To be able to probe this holographic behavior in the laboratory, it is of interest to create a "black hole on a chip" [8–10], that is, to realize the SYK model in the solid state. Reference [8] proposed to use a quantum dot formed by an opening in a superconducting sheet on the surface of a topological insulator. In a perpendicular magnetic field the quantum dot can trap vortices, each of which contains a Majorana zero mode [11]. Chiral symmetry ensures that the band only broadens as a result of four-Majorana-fermion terms in the Hamiltonian, a prerequisite for the real-valued SYK model. A similar construction uses an array of Majorana nanowires coupled to a quantum dot [9]. Since it might be easier to start from conventional electrons rather than Majorana fermions, Ref. [10] suggested to work with the complex-valued SYK model of interacting Dirac fermions in the zeroth Landau level of a graphene quantum dot. Chiral symmetry at the charge-neutrality point again suppresses broadening of the band by two-fermion terms.

The natural way to study a quantum dot is via transport properties. Electrical conduction through chains of SYK quantum dots has been studied in Refs. [12–19]. For a single quantum dot coupled to a tunnel contact, as in Fig. 1, Refs. [8–10] studied the limit of negligibly small coupling strength Γ, in which the differential conductance $G = dI/dV$ equals the density of states of the quantum dot. Conformal symmetry in the large-N limit gives a low-voltage divergence $\propto 1/\sqrt{V}$, until eV drops below the single-particle level spacing $\delta \simeq J/N$ [20–22].

Here we investigate how a finite Γ affects the tunneling spectroscopy. We focus on the complex-valued SYK model for Dirac fermions, as in the graphene quantum dot of Ref. [10]. Our key result is that in the large-N conformal symmetry regime $J/N \ll eV \ll J$ the zero-temperature differential conductance of the quantum dot depends on Γ, J, and V only via the dimensionless combination $\xi = eVJ/\Gamma^2$. Low and high voltages are related by the duality $G(\xi) = G(\pi/\xi)$, providing an experimental signature of the conformal symmetry.

Tunneling Hamiltonian. We describe the geometry of Fig. 1 by the Hamiltonian

$$H = H_{\rm SYK} + \sum_p \varepsilon_p \psi_p^\dagger \psi_p + \sum_{i,p} (\lambda_i c_i^\dagger \psi_p + \lambda_i^* \psi_p^\dagger c_i),$$
$$H_{\rm SYK} = (2N)^{-3/2} \sum_{ijkl} J_{ij;kl}\, c_i^\dagger c_j^\dagger c_k c_l, \tag{1}$$
$$J_{ij;kl} = J_{kl;ij}^* = -J_{ji;kl} = -J_{ij;lk}.$$

The annihilation operators c_i, $i = 1, 2, \ldots$ represent the $N = h\Phi/e$ interacting Dirac fermions in the spin-polarized zeroth Landau level of the graphene quantum dot (enclosing a flux Φ). Two-fermion terms $c_i^\dagger c_j$ are suppressed by chiral symmetry when the Fermi level $\mu = 0$ is at the charge-neutrality point (Dirac point) [10]. The operators ψ_p represent electrons at momentum p in the single-channel lead (dispersion $\varepsilon_p = p^2/2m$, linearized near the Fermi level), coupled to mode i in the quantum dot with complex amplitude λ_i. The tunneling current depends only on the sum of $|\lambda_i|^2$, via the coupling strength

$$\Gamma = \pi \rho_{\rm lead} \sum_i |\lambda_i|^2, \quad \rho_{\rm lead} = (2\pi\hbar v_{\rm F})^{-1}. \tag{2}$$

If $\mathcal{T} \in (0, 1)$ is the transmission probability into the quantum dot, one has $\Gamma \simeq \mathcal{T} N\delta \simeq \mathcal{T} J$.

The Hamiltonian $H_{\rm SYK}$ is the complex-valued SYK model [4] if we take random couplings $J_{ij;kl}$ that are independently distributed Gaussians with zero mean $\langle J_{ij;kl}\rangle = 0$ and variance $\langle |J_{ij;kl}|^2\rangle = J^2$. The zeroth Landau level then broadens into a band of width J, corresponding to a single-particle level spacing $\delta \simeq J/N$ (more precisely, $\delta \simeq J/N \ln N$) [20]. In the energy range $\delta \ll \varepsilon \ll J$ the retarded Green's functions can

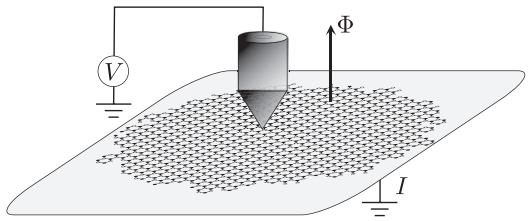

FIG. 1. Tunneling spectroscopy of a graphene flake, in order to probe the complex-valued SYK model [10]. We calculate the current I driven by a voltage V through a single-channel point contact (coupling strength Γ) into a graphene flake on a grounded conducting substrate. At the charge neutrality point a chiral symmetry ensures that the zeroth Landau level (degeneracy $N = e\Phi/h$ for an enclosed flux Φ) is only broadened by electron-electron interactions (strength J). For a sufficiently random boundary the quantum dot can be described by the SYK Hamiltonian (1).

be evaluated in saddle-point approximation [4],

$$G^{\rm R}(\varepsilon) = -i\pi^{1/4}\sqrt{\frac{\beta}{2\pi J}}\,\frac{\Gamma(1/4 - i\beta\varepsilon/2\pi)}{\Gamma(3/4 - i\beta\varepsilon/2\pi)}, \tag{3}$$

where $\beta = 1/k_{\rm B}T$ and $\Gamma(x)$ is the gamma function. At zero temperature this simplifies to

$$G^{\rm R}(\varepsilon) = -i\pi^{1/4}\exp\left[\tfrac{1}{4}i\pi\,{\rm sgn}(\varepsilon)\right]|J\varepsilon|^{-1/2}. \tag{4}$$

Quantum fluctuations around the saddle point cut off the low-ε divergence for $|\varepsilon| < \delta$ [20–22].

Tunneling current. The quantum dot is strongly coupled to a grounded substrate [23], so the current is entirely determined by the transmission of electrons through the point contact. The current operator $\boldsymbol{I}$ is given by the commutator

$$\boldsymbol{I} = \frac{ie}{\hbar}\left[H, \sum_p \psi_p^\dagger \psi_p\right] = i\frac{e}{\hbar}\sum_{n,p}(\lambda_n c_n^\dagger \psi_p - \lambda_n^* \psi_p^\dagger c_n). \tag{5}$$

We calculate the time-averaged expectation value of $\boldsymbol{I}$ using the Keldysh path integral technique [24–27], which has previously been applied to the SYK model in Refs. [12,14,18,28]. The expectation value I of the tunneling current is given by the first derivative of cumulant generating function [25]:

$$I = -i\lim_{\chi\to 0}\frac{\partial}{\partial\chi}\ln Z(\chi), \tag{6}$$

$$Z(\chi) = \left\langle \mathcal{T}_C \exp\left(-i\int_C dt\left[H + \frac{1}{2}\chi(t)\boldsymbol{I}\right]\right)\right\rangle. \tag{7}$$

Here $\mathcal{T}_C$ indicates time-ordering along the Keldysh contour [24] of the counting field $\chi(t)$, equal to $+\chi$ on the forward branch of the contour (from $t = 0$ to $t = \infty$) and equal to $-\chi$ on the backward branch (from $t = \infty$ to $t = 0$). The calculation is worked out in the Appendix.

The result for the differential conductance is

$$G = \frac{dI}{dV} = \frac{e^2}{h}\int_{-\infty}^{+\infty} d\varepsilon\, f'(\varepsilon - eV)\frac{4\Gamma\,{\rm Im}\,G^{\rm R}(\varepsilon)}{|1 + i\Gamma G^{\rm R}(\varepsilon)|^2}, \tag{8}$$

where $f(\varepsilon) = (1 + e^{\beta\varepsilon})^{-1}$ is the Fermi function. Substitution of the conformal Green's function (3) gives upon integration the finite temperature curves plotted in Fig. 2.

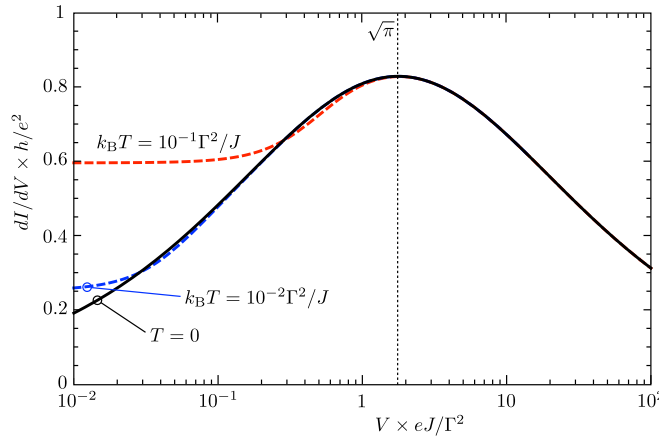

FIG. 2. Differential conductance $G = dI/dV$ calculated from Eq. (8), as a function of dimensionless voltage $\xi = eVJ/\Gamma^2$ for three different temperatures. On the semilogarithmic scale the duality between low and high voltages shows up as a reflection symmetry along the dotted line (where $\xi = \sqrt{\pi}$).

At zero temperature $f'(\varepsilon - eV) \to -\delta(\varepsilon - eV)$ and substitution of Eq. (4) produces a single-parameter function of $\xi = eVJ/\Gamma^2$,

$$G(\xi) = \frac{e^2}{h}\frac{2\sqrt{2}}{\sqrt{2} + \pi^{1/4}\xi^{-1/2} + \pi^{-1/4}\xi^{1/2}}. \tag{9}$$

Low-high voltage duality. The $T = 0$ differential conductance (9) in the conformal regime $J/N \ll eV \ll J$ satisfies the duality relation

$$G(\xi) = G(\pi/\xi), \quad \text{if } N^{-1}(J/\Gamma)^2 \ll \xi, \quad 1/\xi \ll (J/\Gamma)^2. \tag{10}$$

The V-to-$1/V$ duality is visible in the semilogarithmic Fig. 2 by a reflection symmetry of the differential conductance along the $\xi = \sqrt{\pi}$ axis. The symmetry is precise at $T = 0$, and is broken in the tails with increasing temperature.

The voltage range in which V and $1/V$ are related by Eq. (10) covers the full conformal regime for $N \simeq (J/\Gamma)^4$. In this voltage range the $1/\sqrt{V}$ tail at high voltages crosses over to a $\sqrt{V}$ decay at low voltages. The high-voltage tail reproduces the $1/\sqrt{V}$ differential conductance that follows [8–10] from the density of states in the limit $\Gamma \to 0$ (since $\xi \to \infty$ for $\Gamma \to 0$). The density of states gives [20–22] a crossover to a $\sqrt{V}$ decay when eV drops below the single-particle level spacing $\delta \simeq J/N$. Our finite-Γ result (9) implies that this crossover already sets in at larger voltages $eV \simeq \Gamma^2/J$, well above δ for $N \gg (J/\Gamma)^2$.

The symmetrically peaked profile of Fig. 2 is a signature of conformal symmetry in as much as this produces a power-law singularity in the retarded propagator at low energies. It is not specific for the square-root singularity (4); other exponents would give a qualitatively similar low-high voltage duality. For example, the generalized SYK$_{2p}$ model with $2p \geqslant 4$ interacting Majorana fermion terms has a $\varepsilon^{(1-p)/p}$ singularity [5,13], corresponding to the duality $G(\xi_p) = G(C_p/\xi_p)$ with C_p a numerical coefficient and $\xi_p = (eV)^{2(p-1)/p}J^{2/p}\Gamma^{-2}$. In contrast, a disordered Fermi liquid such as the noninteracting SYK$_2$ model, with Hamiltonian $H = \sum_{ij} J_{ij}c_i^\dagger c_j$, has a

constant propagator at low energies and hence a constant dI/dV in the range $J/N \ll eV \ll J$.

Conclusion. We have shown that tunneling spectroscopy can reveal a low-high voltage duality in the conformal regime of the Sachdev-Ye-Kitaev model of N interacting Dirac fermions. A physical system in which one might search for this duality is the graphene quantum dot in the lowest Landau level, proposed by Chen *et al.* [10].

As argued by those authors, one should be able to reach N of order 10^2 for laboratory magnetic-field strengths in a submicrometer-size quantum dot. This leaves two decades in the conformal regime $J/N \ll eV \ll J$. If we tune the tunnel coupling strength near the ballistic limit $\Gamma \lesssim J$, it should be possible even for these moderately large values of N to achieve $N \simeq (J/\Gamma)^4$ and access the duality over two decades of voltage variation. For such large Γ the condition on temperature, $k_B T \ll \Gamma^2/J$, would then also be within experimental reach ($J \simeq 34$ meV from Ref. [10] and $\Gamma \simeq 10$ meV has $k_B T = 10^{-2}\,\Gamma^2/J$ at $T = 300$ mK).

Acknowledgments. We have benefited from discussions with K. E. Schalm and A. Romero Bermudez. This research was supported by the Netherlands Organization for Scientific Research (NWO/OCW) and by an ERC Synergy Grant.

APPENDIX: OUTLINE OF THE CALCULATION

We describe the calculation leading to Eq. (8) for the current-voltage characteristics, generalizing it to nonzero chemical potential μ and including also the shot-noise power. We set $\hbar$ and e to unity, except for the final formulas.

1. Generating function of counting statistics

Arbitrary cumulants of the current operator (5) can be obtained from the generating function (7). A gauge transformation allows us to write equivalently

$$Z(\chi) = \left\langle \mathcal{T}_C \exp\left(-i\int_C H(t)dt\right)\right\rangle, \tag{A1}$$

$$H(t) = H_{\rm SYK} + \sum_p \varepsilon_p \psi_p^\dagger \psi_p - \mu \sum_n c_n^\dagger c_n + \sum_{n,p} (e^{i\chi(t)/2}\lambda_n c_n^\dagger \psi_p + e^{-i\chi(t)/2}\lambda_n^* \psi_p^\dagger c_n). \tag{A2}$$

For generality we have added a chemical potential term $\propto \mu$. (In the main text we take $\mu = 0$, corresponding to a quantum dot at charge neutrality.)

We need the advanced and retarded Green's functions $G^{\rm A}(\varepsilon) = [G^{\rm R}(\varepsilon)]^*$ and the Keldysh Green's function

$$G^{\rm K}(\varepsilon) = \mathcal{F}(\varepsilon)[G^{\rm R}(\varepsilon) - G^{\rm A}(\varepsilon)], \quad \mathcal{F}(\varepsilon) = \tanh(\beta\varepsilon/2). \tag{A3}$$

These are collected in the matrix Green's function $\mathcal{G}$, which on the Keldysh contour has the representation [26,27,29]

$$\mathcal{G} = \begin{pmatrix} G^{\rm R} & G^{\rm K} \\ 0 & G^{\rm A}\end{pmatrix} = L\sigma_3 \begin{pmatrix} G^{++} & G^{+-} \\ G^{-+} & G^{--}\end{pmatrix} L^\dagger, \tag{A4}$$

$$L = \frac{1}{\sqrt{2}}\begin{pmatrix} 1 & -1 \\ 1 & 1\end{pmatrix}, \quad \sigma_3 = \begin{pmatrix} 1 & 0 \\ 0 & -1\end{pmatrix}, \tag{A5}$$

in terms of the Green's functions on the forward and backward branches of the contour:

$$G^{++}(t,t') = -iN^{-1}\sum_n \langle \mathcal{T} c_n(t) c_n^\dagger(t')\rangle, \tag{A6a}$$

$$G^{+-}(t,t') = iN^{-1}\sum_n \langle c_n^\dagger(t') c_n(t)\rangle, \tag{A6b}$$

$$G^{-+}(t,t') = -iN^{-1}\sum_n \langle c_n(t) c_n^\dagger(t')\rangle, \tag{A6c}$$

$$G^{--}(t,t') = -iN^{-1}\sum_n \langle \mathcal{T}^{-1} c_n(t) c_n^\dagger(t')\rangle. \tag{A6d}$$

The operators $\mathcal{T}$ and $\mathcal{T}^{-1}$ order the times in increasing and decreasing order, respectively.

2. Saddle-point solution

In the regime $J/N \ll \varepsilon \ll J$ the Green's function of the SYK model is given by the saddle-point solution [4]

$$G^{\rm R}(\varepsilon) = -iCe^{-i\theta}\sqrt{\frac{\beta}{2\pi J}}\,\frac{\Gamma\left(\frac{1}{4} - i\frac{\beta\varepsilon}{2\pi} + i\mathcal{E}\right)}{\Gamma\left(\frac{3}{4} - i\frac{\beta\varepsilon}{2\pi} + i\mathcal{E}\right)}, \tag{A7}$$

with the definitions

$$e^{2\pi\mathcal{E}} = \frac{\sin\left(\frac{\pi}{4}+\theta\right)}{\sin\left(\frac{\pi}{4}-\theta\right)}, \quad C = (\pi/\cos 2\theta)^{1/4}. \tag{A8}$$

The angle $\theta \in (-\pi/4, \pi/4)$ is a spectral asymmetry angle [30], determined by the charge per site $\mathcal{Q} \in (-1/2, 1/2)$ on the quantum dot according to [31]

$$\mathcal{Q} = N^{-1}\sum_i \langle c_i^\dagger c_i\rangle - \frac{1}{2} = -\theta/\pi - \frac{1}{4}\sin 2\theta. \tag{A9}$$

For $\mu = 0$, when $\mathcal{Q} = 0$, one has $\theta = 0$, $C = \pi^{1/4}$. In good approximation (accurate within 15%),

$$\theta \approx -\tfrac{1}{2}\pi\mathcal{Q} \Rightarrow C \approx (\pi/\cos\pi\mathcal{Q})^{1/4}. \tag{A10}$$

In the mean-field approach the quartic SYK interaction (1) is replaced by a quadratic one with the kernel $\mathcal{G}^{-1}$ from Eq. (A4). A Gaussian integration over the Grassmann fields gives the generating function

$$\ln Z = \int_{-\infty}^{\infty}\frac{d\varepsilon}{2\pi}\ln\left(\frac{\det[1-\Gamma\Xi(\varepsilon)\Lambda^\dagger\mathcal{G}(\varepsilon)\Lambda]}{\det[1-\Gamma\Xi(\varepsilon)\mathcal{G}(\varepsilon)]}\right),$$
$$\Lambda = \begin{pmatrix} \cos(\chi/2) & i\sin(\chi/2) \\ i\sin(\chi/2) & \cos(\chi/2)\end{pmatrix}, \tag{A11}$$
$$\Xi(\varepsilon) = -i\begin{pmatrix} 1 & 2\mathcal{F}(\varepsilon - V) \\ 0 & -1\end{pmatrix}.$$

The matrix $\Xi(\varepsilon)$ is the Keldysh Green's function of the lead, integrated over the momenta. This evaluates

further to

$$\ln Z = \int_{-\infty}^{\infty} \frac{d\varepsilon}{2\pi} \ln\left[1 + \frac{i\Gamma(G^{\rm R} - G^{\rm A})}{(1 + i\Gamma G^{\rm R})(1 - i\Gamma G^{\rm A})}([1 - \mathcal{F}(\varepsilon)\mathcal{F}(\varepsilon - V)](\cos\chi - 1) + i[\mathcal{F}(\varepsilon) - \mathcal{F}(\varepsilon - V)]\sin\chi)\right]. \quad \text{(A12)}$$

At zero temperature the distribution function simplifies to $\mathcal{F}(\varepsilon) \mapsto \mathrm{sgn}(\varepsilon)$, hence

$$\ln Z = \int_{0}^{V} \frac{d\varepsilon}{2\pi} \ln\left[1 + \frac{2i\Gamma(G^{\rm R} - G^{\rm A})(e^{i\chi} - 1)}{(1 + i\Gamma G^{\rm R})(1 - i\Gamma G^{\rm A})}\right]. \quad \text{(A13)}$$

3. Average current and shot-noise power

A p-fold differentiation of $Z(\chi)$ with respect to χ gives the pth cumulant of the current. In this way the full counting statistics of the charge transmitted through the quantum dot can be calculated [25]. The first cumulant, the time-averaged current I from Eq. (6), is given by

$$I = \frac{e}{h}\int_{-\infty}^{+\infty} d\varepsilon\, \frac{i\Gamma[\mathcal{F}(\varepsilon) - \mathcal{F}(\varepsilon - V)](G^{\rm R} - G^{\rm A})}{(1 + i\Gamma G^{\rm R})(1 - i\Gamma G^{\rm A})}, \quad \text{(A14)}$$

which is Eq. (8) from the main text.

At zero temperature the differential conductance $G = dI/dV$ is

$$G(\xi) = \frac{2e^2}{h}\left[1 + \frac{1}{2\sin(\pi/4 + \theta)}\left(\frac{\sqrt{\xi}}{C} + \frac{C}{\sqrt{\xi}}\right)\right]^{-1}, \quad \text{(A15)}$$

with $\xi = eVJ/\Gamma^2$. The duality relation

$$G(\xi) = G(C^4/\xi) \quad \text{(A16)}$$

reduces to the one from the main text, $G(\xi) = G(\pi/\xi)$, when we set $\mu = 0 \Rightarrow \theta = 0 \Rightarrow C = \pi^{1/4}$.

The second cumulant, the shot-noise power P, follows similarly from

$$P = -\lim_{\chi\to 0} \frac{\partial^2}{\partial\chi^2} \ln Z(\chi). \quad \text{(A17)}$$

The Fano factor F, being the ratio of the shot-noise power and the current at zero temperature, is simply given by

$$F = \frac{dP/dV}{dI/dV} = e\left(1 - \frac{h}{e^2}G\right). \quad \text{(A18)}$$

It has the same one-parameter scaling and duality as G. The fact that higher order cumulants of the current have the same scaling as the differential conductance is a consequence of the single-point-contact geometry, with a single counting field $\chi(t)$. This does not carry over to a two-point-contact geometry.

[1] A. Kitaev, A simple model of quantum holography, KITP Program: Entanglement in Strongly-Correlated Quantum Matter (Apr 6 - Jul 2, 2015).

[2] S. Sachdev and J. Ye, Gapless Spin-Fluid Ground State in a Random Quantum Heisenberg Magnet, Phys. Rev. Lett. **70**, 3339 (1993).

[3] S. Sachdev, Holographic Metals and the Fractionalized Fermi Liquid, Phys. Rev. Lett. **105**, 151602 (2010).

[4] S. Sachdev, Bekenstein-Hawking Entropy and Strange Metals, Phys. Rev. X **5**, 041025 (2015).

[5] J. Maldacena and D. Stanford, Remarks on the Sachdev-Ye-Kitaev model, Phys. Rev. D **94**, 106002 (2016).

[6] J. Polchinski and V. Rosenhaus, The spectrum in the Sachdev-Ye-Kitaev model, J. High Energy Phys. 04 (2016) 001.

[7] A. Kitaev and S. J. Suh, The soft mode in the Sachdev-Ye-Kitaev model and its gravity dual, J. High Energy Phys. 05 (2018) 183.

[8] D. I. Pikulin and M. Franz, Black Hole on a Chip: Proposal for a Physical Realization of the SYK Model in a Solid-State System, Phys. Rev. X **7**, 031006 (2017).

[9] A. Chew, A. Essin, and J. Alicea, Approximating the Sachdev-Ye-Kitaev model with Majorana wires, Phys. Rev. B **96**, 121119(R) (2017).

[10] A. Chen, R. Ilan, F. de Juan, D. I. Pikulin, and M. Franz, Quantum Holography in a Graphene Flake with an Irregular Boundary, Phys. Rev. Lett. **121**, 036403 (2018).

[11] L. Fu and C. L. Kane, Superconducting Proximity Effect and Majorana Fermions at the Surface of a Topological Insulator, Phys. Rev. Lett. **100**, 096407 (2008).

[12] X.-Y. Song, C.-M. Jian, and L. Balents, Strongly Correlated Metal Built from Sachdev-Ye-Kitaev Models, Phys. Rev. Lett. **119**, 216601 (2017).

[13] R. A. Davison, W. Fu, A. Georges, Y. Gu, K. Jensen, and S. Sachdev, Thermoelectric transport in disordered metals without quasiparticles: The Sachdev-Ye-Kitaev models and holography, Phys. Rev. B **95**, 155131 (2017).

[14] P. Zhang, Dispersive SYK model: Band structure and quantum chaos, Phys. Rev. B **96**, 205138 (2017).

[15] Y. Gu, X.-L. Qi, and D. Stanford, Local criticality, diffusion and chaos in generalized Sachdev-Ye-Kitaev models, J. High Energy Phys. 05 (2017) 125.

[16] X. Chen, R. Fan, Y. Chen, H. Zhai, and P. Zhang, Competition between Chaotic and Non-Chaotic Phases in a Quadratically Coupled Sachdev-Ye-Kitaev Model, Phys. Rev. Lett. **119**, 207603 (2017).

[17] D. Ben-Zion and J. McGreevy, Strange metal from local quantum chaos, Phys. Rev. B **97**, 155117 (2018).

[18] A. Haldar, S. Banerjee, and V. B. Shenoy, Higher-dimensional SYK non-Fermi liquids at Lifshitz transitions, Phys. Rev. B **97**, 241106 (2018).

[19] Y. Zhong, Periodic Anderson model meets Sachdev-Ye-Kitaev interaction: A solvable playground for heavy fermion physics, arXiv:1803.09417.

[20] D. Bagrets, A. Altland, and A. Kamenev, Sachdev-Ye-Kitaev model as Liouville quantum mechanics, Nucl. Phys. B **911**, 191 (2016).

[21] D. Bagrets, A. Altland, and A. Kamenev, Power-law out of time order correlation functions in the SYK model, Nucl. Phys. B **921**, 727 (2017).

[22] A. V. Lunkin, K. S. Tikhonov, and M. V. Feigel'man, SYK model with quadratic perturbations: The route to a non-Fermi-liquid, arXiv:1806.11211.

[23] We assume that the grounded substrate does not spoil the non-Fermi-liquid state of the quantum dot. This might happen if the coupling becomes too strong, according to S. Banerjee and E. Altman, Solvable model for a dynamical quantum phase transition from fast to slow scrambling, Phys. Rev. B **95**, 134302 (2017).

[24] L. V. Keldysh, Diagram technique for nonequilibrium processes, Sov. Phys. JETP **20**, 1018 (1965).

[25] L. S. Levitov, H.-W. Lee, and G. B. Lesovik, Electron counting statistics and coherent states of electric current, J. Math. Phys. **37**, 4845 (1996).

[26] A. Kamenev and A. Levchenko, Keldysh technique and non-linear σ-model: Basic principles and applications, Adv. Phys. **58**, 197 (2009).

[27] A. Kamenev, *Field Theory of Non-Equilibrium Systems* (Cambridge University Press, Cambridge, UK, 2011).

[28] A. Eberlein, V. Kasper, S. Sachdev, and J. Steinberg, Quantum quench of the Sachdev-Ye-Kitaev Model, Phys. Rev. B **96**, 205123 (2017).

[29] A. I. Larkin and Yu. N. Ovchinnikov, Nonlinear conductivity of superconductors in the mixed state, Sov. Phys. JETP **41**, 960 (1975).

[30] O. Parcollet, A. Georges, G. Kotliar, and A. Sengupta, Overscreened multichannel SU(N) Kondo model: Large-N solution and conformal field theory, Phys. Rev. B **58**, 3794 (1998).

[31] A. Georges, O. Parcollet, and S. Sachdev, Quantum fluctuations of a nearly critical Heisenberg spin glass, Phys. Rev. B **63**, 134406 (2001).